

Dynamical screening of van der Waals interactions in nanostructured solids: Sublimation of fullerenes

Jianmin Tao, Jing Yang, and Andrew M. Rappe

Citation: *The Journal of Chemical Physics* **142**, 164302 (2015); doi: 10.1063/1.4918761

View online: <http://dx.doi.org/10.1063/1.4918761>

View Table of Contents: <http://scitation.aip.org/content/aip/journal/jcp/142/16?ver=pdfcov>

Published by the [AIP Publishing](#)

Articles you may be interested in

[Van der Waals coefficients beyond the classical shell model](#)

J. Chem. Phys. **142**, 024312 (2015); 10.1063/1.4905259

[Communication: Non-additivity of van der Waals interactions between nanostructures](#)

J. Chem. Phys. **141**, 141101 (2014); 10.1063/1.4897957

[Band gap and effective mass of multilayer BN/graphene/BN: van der Waals density functional approach](#)

J. Appl. Phys. **115**, 194304 (2014); 10.1063/1.4876336

[Density, structure, and dynamics of water: The effect of van der Waals interactions](#)

J. Chem. Phys. **134**, 024516 (2011); 10.1063/1.3521268

[The van der Waals coefficients between carbon nanostructures and small molecules: A time-dependent density functional theory study](#)

J. Chem. Phys. **131**, 164708 (2009); 10.1063/1.3256238

How can you **REACH 100%**
of researchers at the Top 100
Physical Sciences Universities? (TIMES HIGHER EDUCATION RANKINGS, 2014)

With *The Journal of Chemical Physics*.

AIP | The Journal of
Chemical Physics

THERE'S POWER IN NUMBERS. Reach the world with AIP Publishing.



Dynamical screening of van der Waals interactions in nanostructured solids: Sublimation of fullerenes

Jianmin Tao, Jing Yang, and Andrew M. Rappe

Department of Chemistry, University of Pennsylvania, Philadelphia, Pennsylvania 19104-6323, USA

(Received 18 January 2015; accepted 10 April 2015; published online 23 April 2015)

Sublimation energy is one of the most important properties of molecular crystals, but it is difficult to study, because the attractive long-range van der Waals (vdW) interaction plays an important role. Here, we apply efficient semilocal density functional theory (DFT), corrected with the dynamically screened vdW interaction (DFT + vdW), the Rutgers-Chalmers nonlocal vdW-DF, and the pairwise-based dispersion-corrected DFT-D2 developed by Grimme and co-workers, to study the sublimation of fullerenes. We find that the short-range part, which accounts for the interaction due to the orbital overlap between fullerenes, is negligibly small. Our calculation shows that there exists a strong screening effect on the vdW interaction arising from the valence electrons of fullerenes. On the other hand, higher-order contributions can be as important as the leading-order term. The reasons are that (i) the surface of fullerene molecules is metallic and thus highly polarizable, (ii) the band gap of fullerene solids is small (less than 2 eV), and (iii) fullerene molecules in the solid phase are so densely packed, yielding the high valence electron density and small equilibrium intermolecular distances (the first nearest neighbor distance is only about 10 Å for C₆₀). However, these two effects make opposite contributions, leading to significant error cancellation between these two contributions. We demonstrate that, by considering higher-order contributions and the dynamical screening, the DFT + vdW method can yield sublimation energies of fullerenes in good agreement with reference values, followed by vdW-DF and DFT-D2. The insights from this study are important for a better understanding of the long-range nature of vdW interactions in nanostructured solids. © 2015 AIP Publishing LLC. [<http://dx.doi.org/10.1063/1.4918761>]

I. INTRODUCTION

Sublimation is one of the basic properties of molecular crystals. It is a familiar phenomenon in daily life, such as sublimation of carbon dioxide (dry ice), snow and ice, iodine, and naphthalene (mothballs). This property has been widely used for purification and cooling in laboratory and industry. Nanostructured solids with high sublimation points, such as fullerenes, can be used as rapid cooling materials for rockets.¹ A good knowledge of the long-range van der Waals (vdW) interaction is important for a better understanding and manipulation of sublimation, because intermolecular forces in most molecular solids essentially arise from vdW interactions.² However, calculation of this property presents a major challenge to conventional density functional theory (DFT), due to the absence of the long-range vdW interaction.

The vdW interaction is an important long-range correlation arising from instantaneous collective charge fluctuations at different locations. It is ubiquitous and affects many properties of molecules and solids, such as lattice constants,^{3,4} cohesive⁵ or sublimation energies,⁶ and physisorption.⁷ It also plays an important role in the determination of higher-order structures of biomolecular chains that define their biological activities.⁸

According to second-order perturbation theory, the (non-retarded) vdW energy between well-separated spherical densities takes the asymptotic form of

$$E_{\text{vdW}} = - \sum_{k=3}^{\infty} C_{2k}/d^{2k}, \quad (1)$$

where d is the separation between the centers of two densities, and C_{2k} are the vdW coefficients. In the simulation of the vdW interaction, the main task is the calculation of the vdW coefficients. Many methods have been proposed^{9–12} to evaluate these coefficients. In particular, Becke and Johnson¹³ proposed an exchange-hole dipole moment model which can generate accurate vdW coefficients for atoms¹⁴ (with an error of 3%) and molecules¹⁵ (with an error of less than 10%). Tkatchenko and Scheffler¹⁶ proposed a method for determining intermolecular vdW coefficients, with an error of about 6%. Recently, Tkatchenko *et al.*¹⁷ have extended this method to include non-additive many-body (e.g., 3-body, 4-body) interactions, improving the performance of the Tkatchenko-Scheffler model for nanoscale systems. Tao, Perdew, and Ruzsinszky developed a solid-sphere model for the dynamic multipole polarizability, which generates for free atom pairs C_6 , C_8 , and C_{10} in excellent agreement (3%) with accurate reference values. Grimme and co-workers¹⁸ developed a sophisticated atom pairwise-based dispersion-corrected DFT method (DFT-D), which improves the predictive ability of conventional DFT in quantum chemistry. Starting from the fluctuation-dissipation theorem¹⁹ and expressing the exchange-correlation energy in terms of density-density response function, Langreth and co-workers²⁰ developed a nonlocal correlation functional to account for the long-range vdW interaction. This nonlocal correlation

functional was then combined with a semilocal exchange functional. The combination is called vdW-DF or Rutgers-Chalmers vdW-DF and has been widely used in electronic structure calculations. Recently, many variants^{21–24} of this functional have been proposed, by combining its correlation part with various exchange functionals. However, these combinations do not bring new physics or exact constraints into this exchange-correlation functional but only achieve better error cancellation between exchange and correlation.

With rapid development of vdW corrections in recent years, the applicability of conventional DFT has been greatly extended to a wider class of problems of interest, and considerable progress has been made in electronic structure calculations.^{25–27} The aim of this work is to present a screened vdW correction for nanostructured solids and apply the new DFT + vdW method to study the intermolecular interaction between fullerenes in the solid phase. Fullerenes are nanosized cage molecules that have long been a topic of interest, due to their many remarkable properties and potential applications.¹ Because all carbon atoms are distributed away from the center (cavity) and because the π -electrons are fully delocalized over the molecular skeleton, the polarizability per atom of fullerenes has a strong size-dependence. As such, the vdW coefficients between fullerenes exhibit unusual strong non-additivity. It was shown^{28,29} that the vdW coefficients between large nanoclusters strongly violate the prediction of a simple atom pairwise model. A simple way to avoid this size-dependent deviation is to treat a fullerene molecule as a whole object and the vdW interaction between two fullerene molecules as that between two objects, rather than to decompose a fullerene molecule as individual atoms and treat the vdW interaction between two fullerene molecules as a sum of atom pair interactions, where each pair involves one effective atom from each of the two fullerene molecules. This treatment may not enable us to study the intramolecular interaction, which is relevant to chemical reactions. However, it has great advantages for the study of the properties arising from the intermolecular forces, such as sublimation or cohesive energies and lattice constants.

II. DYNAMICAL SCREENING OF vdW INTERACTION IN SOLIDS

Recently, it has been shown that the vdW coefficients between nanoclusters can be accurately generated from the conducting shell model.²⁸ This model only requires the accurate static dipole polarizability $\alpha_1(0)$ and the average valence electron density as input, while the higher-order static polarizability is estimated from the classical relationship $\alpha_l(0) = [\alpha_1(0)]^{(2l+1)/3}$, which is exact for the uniform electron gas. These requirements can be well satisfied with slowly varying densities, the paradigm of condensed matter physics. As such, the model is particularly well suited for nanostructures, in which the electron density is slowly varying. However, the conducting shell model of Ref. 28 is valid only for isolated nanostructures. For nanostructures in the solid state, the screening of valence electrons of fullerenes must be considered. Let us first consider a quasi-spherical conducting shell of uniform density inside and zero outside the shell, with outer radius of R and

shell thickness t , placed into a uniform continuous medium with the dielectric function $\epsilon_1(iu)$. The conducting shell will develop an instantaneous dipole or multipole moment with the dynamic multipole polarizability $\alpha_l(iu)$. Due to the dielectric screening of the medium, the electric multipole polarizability of the conducting shell in the continuous medium or bulk solid will be reduced, compared to that in empty space. According to Refs. 3, 30, and 31, the screening effect from the medium can be accounted for via the frequency-dependent dielectric function $\epsilon_1(iu)$ of the medium or bulk solid. As a result, the screened dynamic multipole polarizability of the quasi-spherical conducting shell (which models a fullerene molecule in the solid phase) can be written as

$$\alpha_l^{\text{sc}}(iu) = \left(R^{2l+1} \frac{\omega_l^2}{\omega_l^2 + u^2} \frac{1 - \rho_l}{1 - \beta_l \rho_l} \right) \frac{1}{\epsilon_1(iu)}, \quad (2)$$

$$\beta_l = \frac{\omega_l^2 \tilde{\omega}_l^2}{(\omega_l^2 + u^2)(\tilde{\omega}_l^2 + u^2)}, \quad (3)$$

$$\rho_l = \left(\frac{R-t}{R} \right)^{2l+1}, \quad (4)$$

where $\omega_l = \omega_p \sqrt{l/(2l+1)}$ is the plasmon frequency of a solid sphere, $\tilde{\omega}_l = \omega_p \sqrt{(l+1)/(2l+1)}$ is the plasmon frequency of a cavity, with $\omega_p = \sqrt{4\pi n}$ being the plasmon frequency of the extended uniform electron gas, and ρ_l is the shape function. (Atomic units are used unless otherwise explicitly stated.) When the shell thickness $t = R$, the cavity vanishes and the shell becomes a solid sphere. This model is valid for any value of t . The plasmon frequencies of the solid sphere and cavity can be calculated from the average valence electron density in the shell, which is given by $n = N/V$, with N being the number of valence electrons of a fullerene, and $V = (4\pi/3)[R^3 - (R-t)^3]$ being the shell volume. The outer radius R can be calculated from the quantum molecular dynamics.³² The shell thickness t is size-independent. In this work, we take $t = 3.4$ as adopted in Refs. 33 and 34.

From Eq. (2), we can see that the screening effect is frequency-dependent. Fullerenes have highly polarizable quasi-spherical surfaces, and the vdW interactions between them obey a scaling law,^{28,35,36} which is quite different either from that of 2D layered materials³⁷ or 3D. The crystal structure of fullerenes is fcc (or slightly distorted fcc).³⁸ The screening effect on the vdW interaction between fullerene molecules in the solid phase can be accounted for via the isotropic frequency-dependent dielectric function, as in metals and rare-gas solids. The electrostatic field of one fullerene as it fluctuates is fairly long range and affects (and is screened by) many other fullerenes. As such, the anisotropy of each individual fullerene is of little consequence, and the screening can be modeled as spatially uniform with little loss of accuracy. The exact dielectric function is known in two limits: The uniform-gas (simple metal) limit in which $\epsilon_1(iu) = 1 + \tilde{\omega}_p^2/u^2$ and the low-density limit (e.g., in vacuum or perfect insulator), where $\epsilon_1(iu) = 1$. In the uniform-gas limit, electrons are fully delocalized so that the screening effect is maximal, while in the low-density or large energy-gap limit, electrons are highly localized on the objects so that $\epsilon_1(iu) \approx 1$ and screening effect becomes minimum. However, the exact explicit form of $\epsilon_1(iu)$

for inhomogeneous densities is not known. Many models^{39–41} have been proposed to simulate $\epsilon_1(iu)$. In this work, we use the modified Penn model proposed by Breckenridge, Shaw, Jr., and Sher⁴⁰ to account for the dynamical screening. The model takes the simple form⁷

$$\epsilon_1(iu) = 1 + \frac{\bar{\omega}_p^2}{u^2} \left[\frac{(1 - \Delta^2)y}{P} - \frac{\omega_g^2 - (\omega_g^2 + u^2)\Delta^2}{2u\sqrt{\omega_g^2 + u^2}} \ln \frac{I_+}{I_-} \right] + \frac{2\bar{\omega}_p^2\Delta}{u^2} \left\{ \frac{\omega_g}{u} \left[\tan^{-1} \left(\frac{\omega_g P}{u} \right) - \tan^{-1} \left(\frac{\omega_g}{u} \right) \right] + \frac{1}{P} - 1 \right\}, \quad (5)$$

where $I_{\pm} = [(1 + y^2)(1 + u^2/\omega_g^2)]^{1/2} \pm uy/\omega_g$, $y = 1/\Delta$, and $P = (1 + y^2)^{1/2}$. ω_g is the effective energy gap which will be defined below, and $\Delta = \omega_g/4\epsilon_F$, with $\epsilon_F = (3\pi^2\bar{n})^{2/3}/2$ the Fermi energy, and \bar{n} is the average valence electron density of the bulk solid. This model has been used to study the physical adsorption.^{7,42}

To ensure that our $\epsilon_1(iu)$ is realistic, we determine ω_g by reproducing the static dielectric function $\epsilon_1(0)$ with the Penn model,³⁹

$$\epsilon_1(0) = 1 + \frac{\bar{\omega}_p^2}{\omega_g^2} \left[(1 + \Delta^2)^{1/2} - \Delta \right]. \quad (6)$$

Although the model frequency-dependent dielectric function was derived on the basis of the nearly free electron gas, it should be quite realistic, even for densities away from the nearly free electron gas, because the model recovers the correct static limit $\epsilon_1(0)$ of fullerenes by Eq. (6) and infinite-frequency limit as $O(1/u^2)$. Our recent GW calculations⁴³ including exciton effect (by solving the Bethe-Salpeter equation within the GW approximation) for several semiconductors show that the model dielectric function of Eq. (5) agrees reasonably well with the GW values. Fullerenes are semiconductors with band gaps of less than 2 eV (the maximum band gap is 2 eV which occurs for C₆₀). Therefore, good accuracy of the model $\epsilon_1(iu)$ [Eq. (5)] is expected. The $\epsilon_1(0)$ values of fullerenes can be estimated from the accurate static dipole polarizability using the Clausius-Mossotti formula⁴⁴

$$\alpha_l(0) = \frac{3}{4\pi\rho} \frac{\epsilon_1(0) - 1}{\epsilon_1(0) + 2}. \quad (7)$$

Here, ρ is the particle number density of the solid. For the fcc structure, $\rho = 4/a^3$, where a is the lattice constant. The static polarizability can be calculated from time-dependent density functional theory (TDDFT)⁴⁵ or time-dependent Hartree-Fock (TDHF).³⁵ For convenience, all the input parameters $\alpha_l(0)$, $\epsilon_1(0)$, and ω_g are listed in Table I.

III. LATTICE CONSTANT CALCULATION

Now we turn to the lattice constant calculation. Lattice constant is perhaps the most important geometrical parameter in materials science. Accurate prediction of this quantity is of broad interest on its own. In addition, lattice constant is an important input in the present work. While the experimental values for the fullerene solids considered here are

TABLE I. Static dipole polarizabilities (in a.u.) of free fullerene molecules, static dielectric constants, effective energy gaps (in hartree), and conventional unit cell equilibrium lattice constants (in Å) of fullerene solids. All the data are from the present work, except as noted. The higher-order static multipole polarizabilities $\alpha_l(0)$ are estimated from $\alpha_l(0) = [\alpha_1(0)]^{(2l+1)/3}$. M.R.E. = mean relative error.

Fullerene	$\alpha_1(0)$	$\epsilon_1(0)$	ω_g	a^{LDA}	a^{expt}
C ₆₀ (I _h)	537 ^a	3.813	0.444	14.024	14.17 ^b
C ₇₀ (D _{5h})	685 ^a	4.260	0.410	14.837	15.01 ^b
C ₇₆ (D ₂)	756 ^c	4.309	0.405	15.297	15.475 ^b
C ₇₈ (C _{2v})	779 ^a	4.246	0.406	15.498	15.56 ^d
C ₈₄ (D ₂)	837 ^a	4.242	0.406	15.876	16.06 ^b
C ₉₆ (C ₂)	971 ^e	4.233	0.404	16.689	16.83 ^b
M.R.E.					-1%

^aFrom Ref. 35.

^bFrom Ref. 46.

^cInterpolated between C₇₆ and C₇₈.

^dFrom Ref. 47.

^eInterpolated between C₉₀ and C₁₀₀ values evaluated with time-dependent local density approximation (TDLDA).⁴⁵

available in the literature, most theoretical calculations have been devoted to C₆₀ and C₇₀.⁴⁸ To make our calculation predictive, we avoid any experimental input in this work. It was shown⁴⁹ that DFT-LDA (local density approximation) tends to underestimate experimental values, while GGA (generalized gradient approximation⁵⁰) overestimates them. But GGA gives an overall improvement over LDA for normally bonded solids. However, for solids with strong long-range vdW interactions such as many molecular crystals (e.g., fullerenes), LDA is more accurate than GGA for lattice constants. This is because LDA tends to overestimate the short-range attraction,⁵¹ which partly compensates the absence of long-range attraction in semilocal DFT. In this work, we calculate lattice constants with LDA, using the plane wave pseudopotential code Quantum ESPRESSO.⁵² As discussed below, the pseudopotential-based GGA functional⁵⁰ will be used to describe the short-range contribution to the sublimation energy. Here, we generate norm-conserving LDA and GGA pseudopotentials, with the OPIUM program.⁵³ The LDA pseudopotential employs the Perdew-Zunger parametrization⁵⁴ for the correlation part, with energy cutoff $E_{\text{cut}} = 25$ hartree, while the GGA pseudopotential employs the Perdew-Burke-Ernzerhof (PBE) exchange-correlation functional,⁵⁰ with the same energy cutoff.

The LDA pseudopotential is therefore used to optimize the lattice structure of fullerene solids. In our calculations, an $8 \times 8 \times 8$ k -point grid is used. Our calculations show that, except for C₆₀, which has the perfect fcc structure, all other fullerenes give a slightly distorted fcc structure, due to the deviation from spherical symmetry. Consequently, the distortion results in some changes in unit-cell lengths and angles, as shown in Table II. However, except for C₇₀ whose deviation is 1.8°, the deviation of the solid angles for all other fullerenes considered is less than 1°. Therefore, we may treat the distorted lattices as face-centered orthorhombic ($a \neq b \neq c$ and $\alpha = \beta = \gamma = 90^\circ$). As we shall see below, this orthorhombic distortion has a small effect (about 10%) on the sublimation energies. In order to make direct comparison with experimental values,^{46,55,56} in the calculation of the vdW energy with the asymptotic expansion, we use the fcc lattice structure and take

TABLE II. Distorted fcc (dist) lattice structures and the sublimation energies calculated from the distorted lattice structures. Lattice constant (a, b, c) is in angstrom, solid angle of the distorted lattice in parenthesis (α, β, γ) is in degree, and sublimation energy at zero temperature ($\Delta E_{\text{sub}}^{\text{dist}}$) is in kJ/mol. a^{LDA} of Table I is found from $(abc)^{1/3}$, as listed below.

Fullerene	a (α)	b (β)	c (γ)	$\Delta E_{\text{sub}}^{\text{dist}}$
C ₆₀ (I _h)	14.02 (90.0)	14.02 (90.0)	14.02 (90.0)	174
C ₇₀ (D _{5h})	14.07 (91.9)	14.36 (90.1)	16.18 (90.1)	230
C ₇₆ (D ₂)	13.78 (89.9)	15.24 (90.0)	17.05 (90.1)	249
C ₇₈ (C _{2v})	14.35 (90.1)	15.21 (90.0)	17.06 (90.0)	234
C ₈₄ (D ₂)	15.09 (90.0)	15.44 (89.9)	17.18 (90.2)	225
C ₉₆ (C ₂)	15.46 (90.2)	16.60 (90.3)	18.11 (90.9)	227

the geometric mean of the distorted lattice constants. From Table I, we observe that the effective fcc lattice constants are too short by 1%, compared to experiments. This error may carry over to an error of about 6% in sublimation energy.

IV. RESULTS AND DISCUSSION

The sublimation energy is defined as the energy difference between molecules in the gas phase and the solid phase. Many calculations^{48,57} have been performed on C₆₀ and C₇₀, with semilocal DFT and molecular dynamics. In particular, Fernandes *et al.*⁵⁸ calculated the sublimation energies of fullerenes up to C₉₆ at different temperatures with the classical Monte Carlo method based on an intermolecular potential. The calculated sublimation energies of fullerenes are in excellent agreement with experiments. Recently, Berland *et al.* calculated the sublimation energy⁵ of C₆₀ with several variants of the vdW-DF functional. The result sensitively depends on the choice of the exchange part of this functional. In the present work, we employ DFT-GGA corrected with the dynamically screened vdW interaction to study the sublimation energies of the fullerenes for which experimental values are available for comparison: C₆₀, C₇₀, C₇₆, C₇₈, C₈₄, and C₉₆. Sublimation energy comes from two contributions: the short-range part, which can be well described with semilocal DFT, and the long-range part. The short-range part arises from the orbital overlap of two fullerenes. As pointed out in the first paragraph of Sec. III, the LDA tends to overestimate the short-range contribution. Therefore, here we calculate the short-range part with the GGA functional.⁵⁰ From Table III, we observe that the short-range contribution alone is far too small compared

TABLE III. Sublimation energies (in kJ/mol) of fullerene solids calculated with DFT + vdW, DFT-D2, and vdW-DF.

Fullerene	GGA	GGA + vdW	DFT-D2	vdW-DF	$\Delta H_{\text{sub}}^{\text{ref}}$
C ₆₀ (I _h)	7.9	174	148	185	175 ± 14 ^a
C ₇₀ (D _{5h})	7.5	210	164	210	200 ± 6 ^a
C ₇₆ (D ₂)	7.1	213	171	213	206 ± 4 ^a
C ₇₈ (C _{2v})	7.5	208	167	216	207 ^b
C ₈₄ (D ₂)	7.5	208	178	233	225 ± 6 ^a
C ₉₆ (C ₂)	7.9	209	197	251	222 ^b

^aFrom experiments⁵⁹ at 298 K, except for C₆₀ which is at 0 K.

^bEstimated from the classical Monte Carlo values⁵⁸ at 0 K.

to experimental values,⁵⁹ suggesting that there is negligible orbital overlap between fullerenes.

Next, we calculate the long-range part with the asymptotic expression discussed above. This formula is divergent in the small-separation limit, while the exact vdW energy must be finite. To fix this problem, one usually multiplies each term C_{2k}/d^{2k} by a damping function $f(d)$. Here, we apply the asymptotic formula directly to calculate the long-range part, because at equilibrium, the first-nearest intermolecular distance $d = a^{\text{LDA}}/\sqrt{2}$ (18.7, 19.8, 20.4, 20.7, 21.2, and 22.3 for C₆₀, C₇₀, C₇₆, C₇₈, C₈₄, and C₉₆) is always larger than the average effective diameters of fullerenes ($2R = 16.3, 17.6, 18.2, 18.4, 18.8,$ and 19.8) by more than 10%. Applying a damping function⁶⁰ $f_d(d) = 1/\{1 + \exp[-c(d/d_{\text{vdW}} - 1)]\}$, where $c = 23$ and $d_{\text{vdW}} = 2R$ is the sum of the effective radii, only reduces vdW interactions by about 1%. The vdW coefficients between fullerene molecules in the solid phase can be calculated from the screened dynamic multipole polarizability of Eq. (2), with the second-order perturbation theory or Casimir-Polder formula.⁶¹ The long-range part is the sum of the vdW interactions of a fullerene molecule with all other fullerenes in the solid. Due to the huge vdW coefficients and highly densed packing of fullerenes, the higher-order contributions are significantly important and the convergence of the asymptotic series is very slow. In this work, we truncate the series for $k > 16$ (C₃₂). This high order is far beyond the reach of most vdW methods. Then, we sum all these contributions up to the sixth-nearest neighbors. To see the screening effect, we also calculate the unscreened vdW energy. Comparison of the screened vdW coefficients ($C_6, C_8,$ and C_{10}) with the unscreened ones is displayed in Table IV. Our calculations show that, without screening, the vdW energy is dramatically too large. Figure 1 shows the comparison of the screened dynamic dipole polarizabilities with the unscreened ones. From Fig. 1, we can see that the screening effect is very important, in particular in the low-frequency region. From Fig. 1(a), we also see that the model dynamic polarizability agrees reasonably well with the much more expensive Hartree-Fock (HF) values.³⁵ The good agreement of the model dielectric function with the GW values and the unscreened model dynamic polarizability with the HF value suggests the validity of our dynamically screened dynamic dipole polarizability. The sublimation energies can be obtained by adding the short-range part to the long-range contribution. From Table III, we see that the present GGA + vdW sublimation energies agree very well with the

TABLE IV. Comparison of the screened vdW coefficients per atom pair to the unscreened ones between identical fullerene pairs based on the effective fcc structure. Only C₆, C₈, and C₁₀ are listed here. Other higher-order coefficients can be easily generated from the second-order perturbation formula of Ref. 61. hartree atomic units are used.

Fullerene	C ₆	C ₈ /10 ³	C ₁₀ /10 ⁵	C ₆ ^{sc}	C ₈ ^{sc} /10 ³	C ₁₀ ^{sc} /10 ⁵
C ₆₀ (I _h)	40.83	15.08	45.79	8.876	3.499	11.15
C ₇₀ (D _{5h})	44.20	18.88	66.26	9.681	4.421	16.32
C ₇₆ (D ₂)	45.19	20.66	77.61	9.772	4.788	18.96
C ₇₈ (C _{2v})	45.43	21.20	81.30	9.968	4.984	20.14
C ₈₄ (D ₂)	45.19	22.16	89.28	9.897	5.206	22.13
C ₉₆ (C ₂)	45.48	24.56	109.0	10.12	5.868	27.50

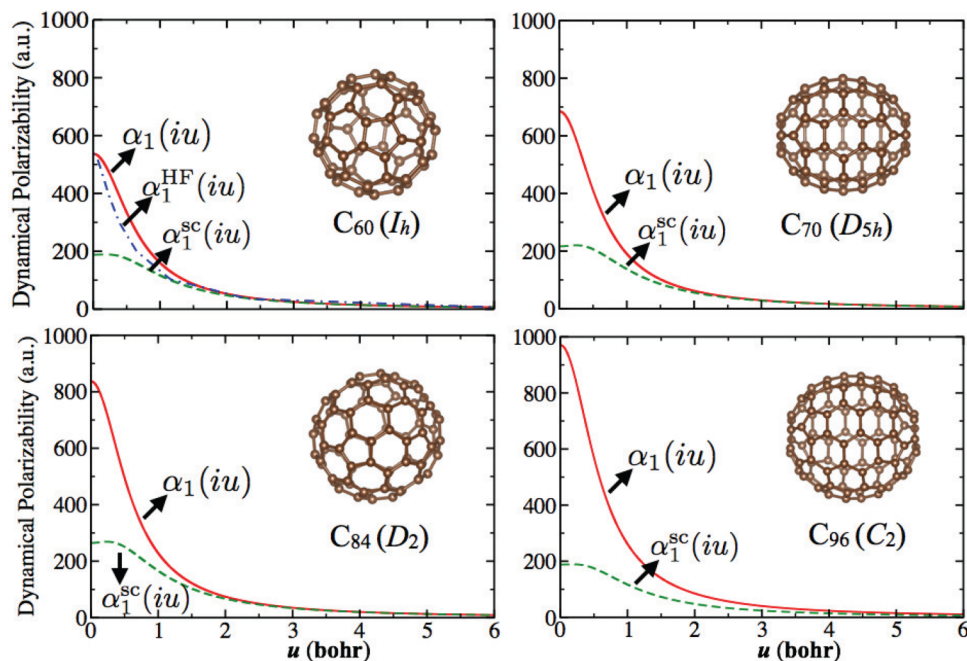


FIG. 1. Comparison of the screened dynamic dipole polarizability $\alpha_1^{\text{sc}}(iu)$ of fullerenes in the solid phase with the dynamic dipole polarizability $\alpha_1(iu)$ of free fullerenes.

reference values. In order to check whether this accuracy is based on the use of the too-short LDA lattice constants, we repeat the calculations with the experimental geometries. From Fig. 2, we observe that these sublimation energies agree well with experiments, too. The good agreement between the sublimation energies calculated with the LDA lattice constants and with experimental lattice constants suggests that the correct physics is indeed built into the model.

Experiment shows that at about 340 K, fullerenes rotate rather freely in the fcc lattice,⁵⁶ while below this temperature, the fullerene lattice is a mixture of fcc and hcp, with very small energy difference (less than 0.1%³⁸) between fcc and hcp. To have a better understanding of this orientation effect,^{48,62} we calculate the long-range vdW energy of a fullerene molecule with all other fullerenes in the effective fcc and distorted fcc structures. We find that the orientation of fullerenes can affect the vdW energy by about 20 kJ/mol on average, via distortion of the lattice, as shown in Table V. This leads to the increase of sublimation energy by about 10% (see Table II).

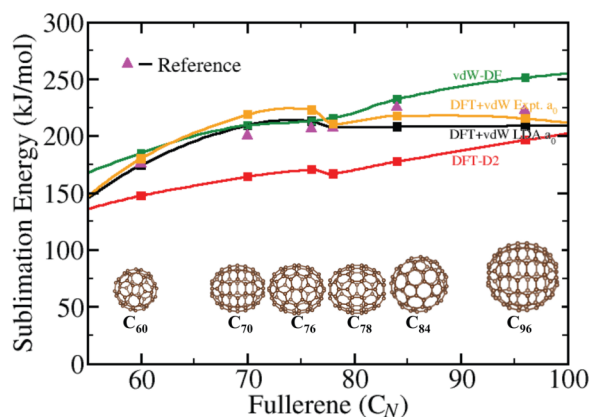


FIG. 2. Sublimation energies of fullerenes calculated with the DFT + vdW, vdW-DF, and DFT-D2 methods. Expt- a_0 represents the sublimation energies with the vdW part calculated from experimental fcc lattice constants.

V. vdW-DF AND DFT-D2 METHODS

To see the performance of other methods, we calculate the sublimation energies of the same fullerenes with the nonlocal vdW-DF and pairwise-based dispersion-corrected DFT-D2 methods, using the Quantum ESPRESSO⁵² code. Since the exchange parts of these two functionals are quite similar (the PBE GGA⁵⁰ in DFT-D2 and the revised version of the PBE GGA in vdW-DF), the same PBE GGA pseudopotential from our short-range calculation was employed here. From Table III, we can see that the DFT + vdW method is slightly more accurate than vdW-DF, while DFT-D2 underestimates the sublimation energies by about 20%. In our DFT + vdW method, the vdW part is constructed with the conducting sphere of uniform density, while the GGA is constructed in the way that is exact in the uniform-gas limit, but only approximately correct for inhomogeneous systems. It includes nearly all-order contributions, while the screening effect is taken into consideration via the frequency-dependent dynamical dielectric function. The dispersion correction in DFT-D2 was based on a sophisticated atom pairwise interaction picture. While it is very accurate for molecules in the gas phase, it may not be optimal for molecules in the solid

TABLE V. Comparison of the long-range contributions (in kJ/mol) to sublimation energy calculated with the effective fcc and distorted fcc lattice structures. If C_{60} is excluded, the mean deviation between the fcc and distorted fcc structures is 23.9 kJ/mol.

Fullerene	vdW(fcc)	vdW(dist)	vdW(dist) – vdW(fcc)
$C_{60}(I_h)$	166.5	166.5	0
$C_{70}(D_{5h})$	202.1	222.6	20.5
$C_{76}(D_2)$	206.3	242.3	36.0
$C_{78}(C_{2v})$	200.4	227.2	26.8
$C_{84}(D_2)$	201.0	218.0	17.2
$C_{96}(C_2)$	201.3	219.7	18.8
Mean deviation			20.1

phase, because there is a strong screening effect, which tends to reduce the vdW interaction. On the other hand, in DFT-D2, only the leading-order (C_6) contribution has been considered. Due to the error cancellation in the dielectric screening and higher-order contribution, the sublimation energies obtained from this method still agree reasonably well with the reference values, as shown in Table III, although it has a tendency to underestimate them. Because the starting point of the vdW-DF is the fluctuation-dissipation theorem,¹⁹ the vdW-DF takes the screening effect into consideration.^{20,63} It was shown⁶⁴ that there is a large error in the vdW-DF vdW coefficients between small molecules. This error should be reduced with increasing system size, because the vdW-DF functional becomes correct for the uniform electron gas. Therefore, vdW-DF can achieve performance similar to that of our screened classical shell model, yielding accurate sublimation energies of fullerenes (see Table III).

Finally, it is worth pointing out that the constructions of these three methods are quite different. Our vdW part is obtained by treating a fullerene molecule as a whole object, while the dispersion part in DFT-D method is atom pairwise-based model, which is calculated by decomposing a fullerene molecule as the sum of individual effective carbon atoms (just opposite to our present method). On the other hand, the nonlocal vdW-DF was based on the density response. These differences make our comparative study immediately helpful for a better understanding of these methods and the physics behind these methods.

VI. CONCLUSION

In conclusion, we have studied the sublimation energies of fullerenes with semilocal DFT, corrected by the dynamically screened vdW interaction. Our calculations show that the sublimation energies of fullerenes essentially arise from the vdW interaction. We find that there is a strong screening effect of valence electrons of fullerenes on the vdW interaction between fullerene molecules in the solid phase. Our calculations also show that the higher-order contribution is very important. If all higher-order terms are neglected, the screened leading-order contribution only accounts for about 20% of the sublimation energy of C_{60} .

The unusually strong screening effect and large higher-order contributions arise from the facts that (i) due to the delocalization of surface electrons, the surface of fullerenes is highly polarizable, (ii) the band gap of fullerene solids is small (less than 2 eV), and (iii) fullerene molecules in the solid phase are so densely packed, leading to small equilibrium intermolecular distance (the first nearest neighbor ≈ 10 Å for C_{60} solid) and high valence electron density. For usual molecular crystals or atomic ion-based solids (e.g., metals and ionic solids), the screening effect of valence electrons and higher-order multipolar components are relatively smaller but still are important, as reported in Refs. 3 and 30. The significance of the higher-order multipolar contribution to the vdW interaction was pointed out in Refs. 65 and 66 for atom pairs, discussed for nanoclusters (no cavity)^{29,67} and for rare-gas atoms on surfaces,⁷ and considered in the third version of Grimme's DFT-D method.¹⁸

To have a better understanding of this and the screening effect, we also performed calculations of the sublimation energies with vdW-DF (popular in solid-state calculations) and DFT-D2 (popular in quantum chemistry), both of which are available in Quantum ESPRESSO.⁵² We find that vdW-DF tends to yield slightly larger but still accurate sublimation energies and thus stronger bonding, while DFT-D2 tends to predict significantly weaker vdW bonding. There is clear evidence of multipole enhancements of the nonlocal-correlation attraction at binding.^{63,68} Recent studies have shown that DFT-D method significantly improves the performance of semilocal DFT for molecular calculations,⁶⁹ but it overcorrects the lattice constants of both ice and AgI.⁷⁰ The reason is that in solids, the screening of valence electrons is much stronger than the screening effect in molecules. Therefore, a vdW method optimal for molecules may not be optimal for solids. Highly delocalized electrons not only produce strong screening effect but also yield strong multipolar components. Strong higher-order multipolar contribution in fullerenes also suggests important unequal contribution of each carbon atom in fullerene molecules.^{28,29} The further away an atom is from the center of a fullerene molecule, the larger the polarizability of that atom is, a similar situation in metallic systems.

Although our present work has focused on the calculation of sublimation energies of fullerenes, it can be used to study other vdW-related properties such as lattice constant and bulk modulus corrections. It can be also used to study other nanostructured solids.

ACKNOWLEDGMENTS

J.T. thanks Bing Xiao for helpful discussions and Wissam Saidi for discussions and for kindly sending his numerical data of the dynamic dipole polarizability of C_{60} (Fig. 3 of Ref. 6) to us. J.T. acknowledges the support of the NSF under Grant No. CHE-1261918 and the Office of Naval Research, under Grant No. N00014-14-1-0761. J.Y. was supported by the NSF under Grant No. CMMI-1334241. A.M.R. was supported by the Department of Energy Office of Basic Energy Sciences, under Grant No. DE-FG02-07ER15920. Computational support was provided by the HPCMO and the NERSC.

¹M. S. Dresselhaus, G. Dresselhaus, and P. C. Eklund, *J. Mater. Res.* **8**, 2054 (1993).

²G. D. Mahan, *J. Chem. Phys.* **43**, 1569 (1965).

³J. Tao, J. P. Perdew, and A. Ruzsinszky, *Phys. Rev. B* **81**, 233102 (2010).

⁴T. Bučko, S. Lebègue, J. Hafner, and J. G. Ángyán, *Phys. Rev. B* **87**, 064110 (2013).

⁵K. Berland, Ø. Borck, and P. Hyldgaard, *Comput. Phys. Commun.* **182**, 1800 (2011).

⁶B. Santra, J. Klimes, D. Alfe, A. Tkatchenko, B. Slater, A. Michaelides, R. Car, and M. Scheffler, *Phys. Rev. Lett.* **107**, 185701 (2011).

⁷J. Tao and A. M. Rappe, *Phys. Rev. Lett.* **112**, 106101 (2014). Note that in curly brackets of Eq. (9), the effective energy gap ω_g was mistyped as ω_p .

⁸R. A. DiStasio, O. A. von Lilienfeld, and A. Tkatchenko, *Proc. Natl. Acad. Sci. U. S. A.* **109**, 14791 (2012).

⁹J. F. Dobson and T. Gould, *J. Phys.: Condens. Matter* **24**, 073201 (2012).

¹⁰J. Tao, J. P. Perdew, and A. Ruzsinszky, *Int. J. Mod. Phys. B* **27**, 1330011 (2013).

¹¹E. J. Meijer and M. Sprk, *J. Chem. Phys.* **105**, 8684 (1996).

¹²E. Tapavicza, I.-C. Lin, O. A. von Lilienfeld, T. Tavernelli, M. D. Coutinho-Neto, and U. Rothlisberger, *J. Chem. Theory Comput.* **3**, 1673 (2007).

¹³A. D. Becke and E. R. Johnson, *J. Chem. Phys.* **122**, 154104 (2005).

¹⁴A. D. Becke and E. R. Johnson, *J. Chem. Phys.* **127**, 154108 (2007).

- ¹⁵S. N. Steinmann and C. Corminboeuf, *J. Chem. Theory Comput.* **7**, 3567 (2011).
- ¹⁶A. Tkatchenko and M. Scheffler, *Phys. Rev. Lett.* **102**, 073005 (2009).
- ¹⁷A. Tkatchenko, R. A. DiStasio, R. Car, and M. Scheffler, *Phys. Rev. Lett.* **108**, 236402 (2012).
- ¹⁸S. Grimme, J. Antony, S. Ehrlich, and H. Krieg, *J. Chem. Phys.* **132**, 154104 (2010).
- ¹⁹M. Fuchs and X. Gonze, *Phys. Rev. B* **65**, 235109 (2002).
- ²⁰M. Dion, H. Rydberg, E. Schröder, D. C. Langreth, and B. I. Lundqvist, *Phys. Rev. Lett.* **92**, 246401 (2004).
- ²¹J. Granatier, P. Lazar, M. Otyepka, and P. Hobza, *J. Chem. Theory Comput.* **7**, 3743 (2011).
- ²²J. Klimes, D. R. Bowler, and A. Michaelides, *Phys. Rev. B* **83**, 195131 (2011).
- ²³K. Berland and P. Hyldgaard, *Phys. Rev. B* **89**, 035412 (2014).
- ²⁴K. Berland, C. A. Arter, V. R. Cooper, K. Lee, B. I. Lundqvist, E. Schröder, T. Thonhauser, and P. Hyldgaard, *J. Chem. Phys.* **140**, 18A539 (2014).
- ²⁵W. A. Al-Saidi, V. K. Voora, and K. D. Jordan, *J. Chem. Theory Comput.* **8**, 1503 (2012).
- ²⁶O. Hod, *J. Chem. Theory Comput.* **8**, 1360 (2012).
- ²⁷D. A. Egger and L. Kronik, *J. Phys. Chem. Lett.* **5**, 2728 (2014).
- ²⁸A. Ruzsinszky, J. P. Perdew, J. Tao, G. I. Csonka, and J. M. Pitarke, *Phys. Rev. Lett.* **109**, 233203 (2012).
- ²⁹J. Tao and J. P. Perdew, *J. Chem. Phys.* **141**, 141101 (2014).
- ³⁰J. J. Rehr, E. Zaremba, and W. Kohn, *Phys. Rev. B* **12**, 2062 (1975).
- ³¹K. K. Mon, N. W. Ashcroft, and G. V. Chester, *Phys. Rev. B* **19**, 5103 (1979).
- ³²G. B. Adams, M. O’Keeffe, and R. S. Ruoff, *J. Phys. Chem.* **98**, 9465 (1994).
- ³³A. A. Lucas, L. Henrard, and Ph. Lambin, *Phys. Rev. B* **49**, 2888 (1994).
- ³⁴G. K. Gueorguiev, J. M. Pacheco, and D. Tománek, *Phys. Rev. Lett.* **92**, 215501 (2004).
- ³⁵J. Kauczor, P. Norman, and W. A. Saidi, *J. Chem. Phys.* **138**, 114107 (2013).
- ³⁶V. V. Gobre and A. Tkatchenko, *Nat. Commun.* **4**, 2341 (2013).
- ³⁷T. Björkman, A. Gulans, A. V. Krasheninnikov, and R. M. Nieminen, *J. Phys.: Condens. Matter* **24**, 424218 (2012).
- ³⁸At room temperature, the crystal structure of C₆₀ is a mixture of fcc and hcp, but the energy difference between the two structures is small (less than 0.1%), as pointed by Ph. Lambin, A. A. Lucas, and J.-P. Vigneron, *Phys. Rev. B* **46**, 1794 (1992).
- ³⁹D. R. Penn, *Phys. Rev.* **128**, 2093 (1962).
- ⁴⁰R. A. Breckenridge, R. W. Shaw, Jr., and A. Sher, *Phys. Rev. B* **10**, 2483 (1974).
- ⁴¹J. T. Foley and U. Landman, *Phys. Rev. B* **14**, 1597 (1976).
- ⁴²G. Vidali and M. W. Cole, *Surf. Sci.* **107**, L374 (1981).
- ⁴³F. Zheng, J. Tao, and A. M. Rappe, “Frequency-dependent dielectric function of semiconductors with application to physisorption” (unpublished).
- ⁴⁴H.-Y. Kim, J. O. Sofo, D. Velegol, M. W. Cole, and G. Mukhopadhyay, *Phys. Rev. A* **72**, 053201 (2005).
- ⁴⁵M. van Faassen, L. Jensen, J. A. Berger, and P. L. de Boeij, *Chem. Phys. Lett.* **395**, 274 (2004).
- ⁴⁶M. N. Magomedov, *High Temp. (USSR)* **43**, 379 (2005).
- ⁴⁷R. D. Bendale and M. C. Zerner, *J. Phys. Chem.* **99**, 13830 (1995).
- ⁴⁸Y. Guo, N. Karasawa, and W. A. Goddard III, *Nature* **351**, 464-467 (1991).
- ⁴⁹P. Haas, F. Tran, and P. Blaha, *Phys. Rev. B* **79**, 085104 (2009).
- ⁵⁰J. P. Perdew, K. Burke, and M. Ernzerhof, *Phys. Rev. Lett.* **77**, 3865 (1996).
- ⁵¹J. Tao and J. P. Perdew, *J. Chem. Phys.* **122**, 114102 (2005).
- ⁵²P. Giannozzi *et al.*, *J. Phys.: Condens. Matter* **21**, 395502 (2009).
- ⁵³A. M. Rappe, K. M. Rabe, E. Kaxiras, and J. D. Joannopoulos, *Phys. Rev. B* **41**, 1227(R) (1990); **44**, 13175 (1991).
- ⁵⁴J. P. Perdew and A. Zunger, *Phys. Rev. B* **23**, 5048 (1981).
- ⁵⁵B. Brunetti, G. Gigli, E. Giglio, V. Piacente, and P. Scardala, *J. Phys. Chem. B* **101**, 10715 (1997).
- ⁵⁶V. I. Zubov, N. P. Tretiakov, and I. V. Zubov, *Eur. Phys. J. B* **17**, 629 (2000).
- ⁵⁷M. R. Pederson and A. A. Quong, *Phys. Rev. Lett.* **74**, 2319 (1995).
- ⁵⁸F. M. S. S. Fernandes, F. F. M. Freitas, and R. P. S. Fartaria, *J. Phys. Chem. B* **107**, 276 (2003).
- ⁵⁹M. Moalem, M. Balooch, A. V. Hamza, and R. S. Ruoff, *J. Phys. Chem.* **99**, 16736 (1995).
- ⁶⁰Q. Wu and W. Yang, *J. Chem. Phys.* **116**, 515 (2002).
- ⁶¹S. H. Patil and K. T. Tang, *J. Chem. Phys.* **106**, 2298 (1997).
- ⁶²Y. Kita, K. Wako, H. Goto, T. Naito, H. Kawai, and I. Okada, *J. Chem. Phys.* **125**, 034506 (2006).
- ⁶³P. Hyldgaard, K. Berland, and E. Schröder, *Phys. Rev. B* **90**, 075148 (2014).
- ⁶⁴Q. A. Vydrovi and T. Van Voorhis, *Phys. Rev. A* **81**, 062708 (2010).
- ⁶⁵J. Mitroy and M. W. J. Bromley, *Phys. Rev. A* **71**, 042701 (2005).
- ⁶⁶J. Tao, J. P. Perdew, and A. Ruzsinszky, *Proc. Natl. Acad. Sci. U. S. A.* **109**, 18 (2012).
- ⁶⁷J. Tao, Y. Fang, P. Hao, G. E. Scuseria, A. Ruzsinszky, and J. P. Perdew, *J. Chem. Phys.* **142**, 024312 (2015).
- ⁶⁸H. Rydberg, M. Dion, N. Jacobson, E. Schröder, P. Hyldgaard, S. I. Simak, D. C. Langreth, and B. I. Lundqvist, *Phys. Rev. Lett.* **91**, 126402 (2003).
- ⁶⁹P. Hao, J. Sun, B. Xiao, A. Ruzsinszky, G. I. Csonka, J. Tao, S. Glindmeyer, and J. P. Perdew, *J. Chem. Theory Comput.* **9**, 355 (2013).
- ⁷⁰Y. Fang, B. Xiao, J. Tao, J. Sun, and J. P. Perdew, *Phys. Rev. B* **87**, 214101 (2013).